

New method for catalyst preparation based on metal-organic framework MOF-5 for the partial hydrogenation of phenylacetylene*

E. V. Belyaeva,^a V. I. Isaeva,^{a} E. E. Said-Galiev,^b O. P. Tkachenko,^a S. V. Savilov,^c
A. V. Egorov,^c L. M. Kozlova,^a V. Z. Sharf,^a and L. M. Kustov^a*

^a*N. D. Zelinsky Institute of Organic Chemistry, Russian Academy of Sciences,
47 Leninsky prosp., 119991 Moscow, Russian Federation.*

Fax: +7 (499) 135 5328. E-mail: sharf@ioc.ac.ru

^b*A. N. Nesmeyanov Institute of Organoelement Compounds, Russian Academy of Sciences,
28 ul. Vavilova, 119991 Moscow, Russian Federation*

^c*Chemical Department, M. V. Lomonosov Moscow State University,
1 Leninskie Gory, 119991 Moscow, Russian Federation*

Small (less than 2 nm) Pd nanoparticles immobilized in the matrix of the microporous phenylencarboxylate metal-organic framework MOF-5 were prepared for the first time by the fluid method. The catalytic properties of samples Pd@MOF-5 were studied in the selective hydrogenation of phenylacetylene to styrene (methanol, 20 °C, $P_{\text{H}_2} = 1$ atm). The catalytic experimental data and results of physicochemical studies indicate that palladium nanoparticles are mostly localized in pores of the composite material 1%Pd@MOF-5 obtained by the fluid synthesis. The specific positions of active sites in the intracrystalline volume results in the suppression of the undesirable conversion of styrene to ethylbenzene.

Key words: metal-organic frameworks, fluid synthesis, partial hydrogenation, phenylacetylene, Pd-containing catalysts, nanoparticles.

Metal nanoparticles as components of active and selective catalysts for various processes are of substantial interest.¹ However, mobility of metal nanoparticles in the processes of nanocomposite preparation results in their aggregation, which prevents the full utilization of their unique properties. In heterogeneous catalysis, the agglomeration of nanoparticles before and after the catalytic reaction can be avoided by immobilizing nanoparticles on the support.^{2,3} Crystalline materials with the ordered structure, such as zeolites and mesoporous silicates, as well as metal-organic coordination polymers (metal-organic frameworks, MOFs), make it possible to stabilize metal nanoparticles by their immobilization in the porous matrix.⁴

The family of MOFs represents hybrid zeolite-like materials formed by metal ions or clusters that are linked by polydentate organic ligands.⁵ A high porosity and high specific surface area, as well as a regular pore size of these systems, create conditions for the uniform size distribution of metal nanoparticles (NPs) in a narrow range and high dispersion of metal-containing catalysts immobilized in the MOF matrix. These properties are interesting for using composites NPs@MOF in heterogeneous catalysis.⁶

Various methods were developed to prepare heterogeneous catalysts of this type: impregnation to incipient wetness, coprecipitation, infiltration of chemical vapors of organometallic compounds with labile ligands into MOF pores (Metal Organic Chemical Vapor Deposition, MOCVD), solid-state mechanical mixing, and consecutive deposition—reduction to form egg-shell type bimetallic particles (for example, Au@Ag).^{7–9} Nanoparticles of Pd, Pt, Fe, Au, Cu, Zn, Sn, Ru, and Ni can be immobilized in the MOF matrices using these methods.^{10–14}

One of the promising methods for preparing heterogeneous catalytic system is the fluid synthesis for which supercritical carbon dioxide (SCF) is used as a solvent. The studies on the synthesis of the Pt/C catalysts for fuel cells^{15–24} and some heterogeneous catalysts^{25,26} in a medium of SCF are known. In the recent time, the fluid synthesis was successfully applied to prepare the ruthenium-containing catalysts based on MOF.^{27,28} The catalysts prepared in the SCF medium are superior to catalytic systems obtained by traditional methods in activity and selectivity.

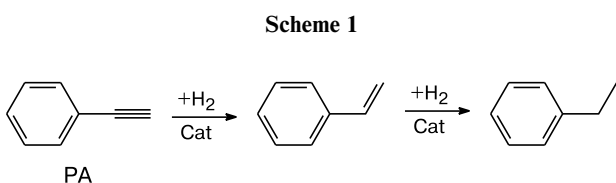
Fluid CO₂ has a series of substantial advantages over liquid solvents. Supercritical CO₂ is characterized by chemical inertness and low critical parameters. Since the interface and, hence, surface tension are absent, SCF has an absolute wettability and does not give capillary effects. Due to these properties, functional additives dissolved in

* On occasion of the 80th anniversary of the N. D. Zelinsky Institute of Organic Chemistry of the Russian Academy of Sciences.

the fluid easily penetrate into pores of polymer, carbon, and inorganic matrices.²⁹

Selective hydrogenation of polyunsaturated compounds has a great applied significance.³⁰ In the industrial scale, the hydrogenation step is a component of hydrofining processes, for instance, acetylene and diene impurities are removed by hydrogenation from olefins.^{31–33} The presence of phenylacetylene in the production of polystyrene exerts a negative effect on the polymerization catalyst and, for this reason, the admissible level of phenylacetylene in polymer is below 10 ppm.³⁴

It should be mentioned that the partial hydrogenation of phenylacetylene (PA) (Scheme 1) is a convenient model reaction for designing novel catalysts.^{35,36} Various catalytic systems were proposed for this reaction: Pd/SiO₂,³⁷ Pd nanoparticles supported on zeolites and mesoporous silicates (MCM-41 and Al-MCM-41)³⁴; amorphous metal alloys (metallic glasses, for example, Pd₈₁Si₁₉)³⁸; and Rh nanoparticles encapsulated into polyvinylpyrrolidone [Rh-PVP].³⁹



In this work, we studied the catalytic properties of the Pd nanoparticles immobilized in the matrix of the phenylencarboxylate metal-organic framework MOF-5 (Zn₄O(BDC)₃, where BDC is benzene-1,4-dicarboxylate). The hydrogenation of phenylacetylene to styrene was chosen as a model reaction. The obtained Pd-containing samples of MOF-5 were characterized by X-ray diffraction analysis, X-ray absorption spectroscopy, scanning electron microscopy (SEM), high-resolution transmission electron microscopy (HR TEM), and measurements of low-temperature nitrogen adsorption.

Experimental

Samples of the microporous metal-organic framework MOF-5 were synthesized according to a previously published procedure.⁴⁰

Preparation of palladium-containing systems. Impregnation to incipient wetness. The Pd-containing samples were prepared using a known procedure.⁷ A solution of palladium acetate (Pd(OAc)₂) or palladium acetylacetonate (Pd(acac)₂) (5.0–50.0 mg, 0.02–0.2 mmol) in absolute chloroform (0.30 mL) was gradually added to the MOF-5 samples (500 mg), and then the solvent was distilled off under reduced pressure. Finally, MOF-5 samples containing the supported precursor Pd(OAc)₂ were evacuated (10^{−3} Torr, 4 h, 150 °C).

Fluid synthesis. Pre-extracted in SCF (70 °C, 15 MPa, 6.5 h) and evacuated samples of the MOF-5 support (0.33 g, 1.4 · 10^{−3} mol)

and Pd(acac)₂ (4.3 mg, 1.4 · 10^{−5} mol) were loaded into a reactor. The reactor was sealed and purged with a flow of dry CO₂ followed by heating the mixture to 150 °C with stirring. Highly pure CO₂ was liquefied in a High Pressure Equipment press and fed to the reactor thus creating a pressure of 10.8 MPa. The reaction mixture was kept under these conditions with stirring for 10 h. Then the reactor was cooled down and depressurized. The second step, metal reduction, was carried out in a flow of dry argon (10–20 cm³ min^{−1}) (220 °C, 4–6 h). Finally, the reactor was cooled down and opened, and the palladium-containing material was dried in a vacuum drying box (80 °C, 2 h).

The palladium content of the synthesized samples was determined on a VRA 30 X-ray fluorescence analyzer (Germany) using the Pd-K α line of the X-ray fluorescence (XRF) spectrum. An X-ray tube with the Mo anode was used in a mode of 50 kV–20 μ A to excite XRF.

Methods of catalyst investigation. The specific surface area of the supports was calculated from the data on nitrogen adsorption using the BET equation.⁴¹ The X-ray diffraction powder patterns were collected on a DRON 3M diffractometer with Cu-K α radiation at a scanning rate of 1 deg min^{−1} ($\lambda = 1.54 \text{ \AA}$).

The XRF spectra were recorded in the transmission mode at 77 K at the Center of Synchrotron Radiation DESY (Hamburg, Germany, project II-2007/0022). The energy positions of the PdK-edge absorption in the XANES Pd/MOFs spectra and Pd foil coincide; however, a comparison of the EXAFS spectra showed that the oscillation intensity in the spectra of the catalysts is much lower and depends on the support.

The microstructure of the samples was studied by field-emission scanning electron microscopy (FE-SEM) on a Hitachi SU8000 electron microscopy. The images were detected in the secondary electron detection mode at an accelerating voltage of 10 kV and a working distance of 8–10 mm. The morphology of the samples was considered with allowance for a correction to the surface effect of conducting layer sputtering.⁴²

The samples were studied by high-resolution transmission electron microscopy on a JEOL JEM 2100F/Cs microscope (JEOL Co. Ltd., Japan). The TEM images were detected at an accelerating voltage of 200 kV and an exposure time of 90 s in the flight-field transmission microscopy mode. When a sample was prepared for analysis, its weighed sample was dispersed for 20 min (20 °C) in water in a Sappfir ultrasonic bath (150 W, 22 kHz). The obtained suspension (100 μ L) was deposited on a copper grid pre-covered with polyvinylformal.

Catalytic experiments. Hydrogenation was carried out in a glass temperature-controlled two-necked reactor with stirring at 800 rpm.

A weighed sample of the catalyst (100 mg, Pd content 1–5%) was saturated with hydrogen for 30 min, and phenylacetylene was introduced (460 mg, 5 mmol). The reaction was carried out in methanol (20 mL) under an atmospheric pressure of H₂ (20 °C).

Experimental verification of the catalyst stability. After completion of the phenylacetylene hydrogenation cycle, the catalyst was removed from the reactor, separated from the reaction solution on a centrifuge, and washed with methanol (2 × 10 mL). Then a fresh portion of methanol (~20 mL) was added, and the system was maintained for 24 h. Then the solvent was removed by decantation, and the catalyst was refluxed for 9 h in methanol (25 mL). The catalyst was isolated on a centrifuge, washed with methanol (2 × 10 mL), and evacuated (4 h, 150 °C, 10^{−2} Torr).

The initial specific rate for hydrogenation of phenylacetylene (W_{01}) and styrene (W_{02}) (mole of substrate (mole of Pd) $^{-1}$ min $^{-1}$) was calculated by the graphical method from the curves describing conversion (<20%) as a function of time. The selectivity at the first step of the hydrogenation process was determined as a ratio of the concentrations of styrene and ethylbenzene in the reaction mixture

$$S = [\text{styrene}] / ([\text{styrene}] + [\text{ethylbenzene}])$$

at the phenylacetylene conversion 50 and 95%.

The GLC analysis was carried out on a Model 3700 chromatograph with a flame-ionization detector on an FFAP capillary column (25 m × 0.25 mm) at 65 °C.

Results and Discussion

Physicochemical study of the synthesized palladium-containing catalysts. The synthesized samples of MOF-5, used as supports for palladium, have high specific surface area (1800–2600 m 2 g $^{-1}$). The X-ray diffraction patterns of the sample of the initial metal-organic framework activated *in vacuo* to remove solvent molecules from pores before palladium deposition and the MOF-5 sample treated in SCF after evacuation are different. The ratio of reflection intensities at small angles (6.9°/9.7°) is higher for the sample additionally treated under the supercritical conditions (Fig. 1). A comparison of the X-ray diffraction pattern of the "supercritical" material with the theoretical X-ray diffraction pattern of MOF-5 shows that the preliminary treatment in SCF before palladium introduction enhances the degree of crystallinity, *i.e.*, improves the quality of the sample of the metal-organic framework. The efficiency of this method for MOF activation for removal of guest molecules from pores was reported earlier for HCC-2.⁴³

The characteristics of the synthesized palladium-containing samples are given in Table 1. The immobilization

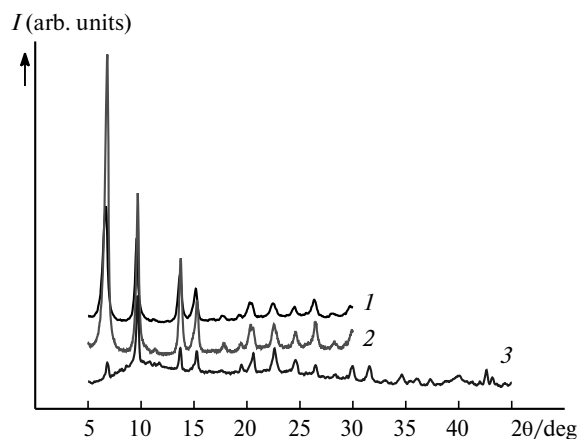


Fig. 1. X-ray diffraction patterns of the initial sample of the metal-organic framework MOF-5 (1), samples MOF-5 after evacuation and additional treatment in SCF (2), and palladium-containing materials V obtained by the fluid synthesis (3).

Table 1. Characteristics of the synthesized palladium-containing samples of the metal-organic framework MOF-5

Catalyst	Preparation method	Precursor	Content of Pd (wt.%)
I	Impregnation	Pd(OAc) $_2$	1.0
II	Impregnation	Pd(OAc) $_2$	5.0
III	Impregnation	Pd(acac) $_2$	1.0
IV	SCF	Pd(acac) $_2$	1.0
V	SCF	Pd(acac) $_2$	3.5

of palladium nanoparticles in the MOF-5 matrix changes the specific surface area of the samples. For example, after Pd was introduced in sample I, the specific surface area decreased by ~280 m 2 g $^{-1}$ compared to the value obtained for the initial metal-organic framework. This decrease seems to indicate a partial localization of palladium nanoparticles inside the cavities of MOF-5.^{44,45} A more noticeable decrease in the specific surface area (by ~1900 m 2 g $^{-1}$) was observed when the amount adsorbed was measured on the Pd/MOF-5 sample prepared from Pd(acac) $_2$ by the impregnation to incipient wetness method.⁷ This significant change in the texture properties can be related to both palladium immobilization in the framework pores and the partial degradation of the structure.

Metal-organic frameworks containing metal nanoparticles are conventionally divided into three classes. Class A (metal/MOF) includes systems with nanoparticles localized on the external surface of microcrystallites of MOF or near the surface. In these systems, the nanoparticle size considerably exceeds the pore dimensions of the metal-organic framework.⁵ Class B (metal@MOFs) is associated with systems containing nanoparticles distributed in the pore volume of MOF microcrystals. Since the size of these particles is larger than pore dimensions, a partial disintegration of the framework occurs. Class C (metal@MOF) represents the systems containing metal nanoparticles immobilized in the microcrystallite bulk of the metal-organic framework. In this case, the average diameter of immobilized nanoparticles is close to or smaller than the pore size.

The X-ray diffraction and SEM studies confirm that the metal-organic framework of the synthesized palladium-containing samples remains unchanged (see Figs 1–3). The cubic topology of the metal-organic framework MOF-5 (with minor changes in the lattice parameter) is retained for samples I and III prepared with the palladium compounds using the impregnation to incipient wetness method (Fig. 2). The experimental X-ray diffraction patterns of palladium-containing samples I and III prepared by the impregnation to incipient wetness method correspond to the theoretical X-ray diffraction pattern of MOF-5 (see Fig. 2). The intensity ratio of the first reflection (6.9°) and second reflection (9.7°) at small angles is ~1.5 in both the

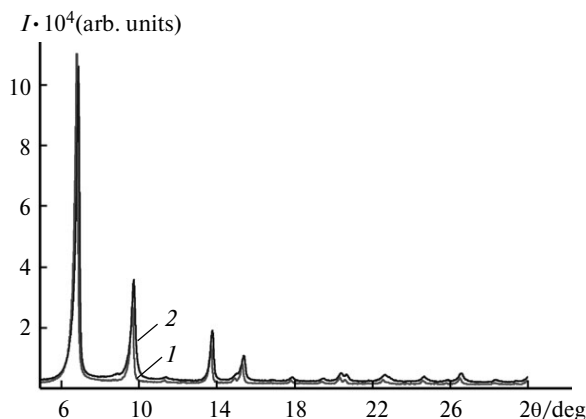


Fig. 2. X-ray diffraction patterns of sample **I** (1) prepared using palladium acetate and sample **III** (2) prepared from palladium acetylacetonate by the impregnation to incipient wetness method.

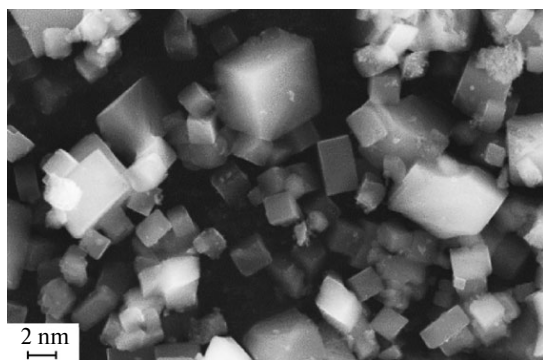


Fig. 3. SEM image of palladium-containing sample **I**.

theoretical diffraction picture of MOF-5 and experimental X-ray diffraction of powders of samples **I** and **III**. However, the X-ray diffraction pattern of sample **V** obtained by the fluid synthesis exhibits the change in the intensity ratio of the characteristic reflections at small angles ($6.9^\circ/9.7^\circ$). It is known that for materials with large pores accessible for solvent and adsorbate molecules the X-ray reflection intensities at angles below 20° (2θ) depend substantially on the amount and ability to X-ray scattering of the particles in pores.⁴⁶ Thus, a decrease in the intensity of the peak at 6.9° relatively to the reflection 9.7° in the X-ray diffraction pattern of sample **V** (synthesis in SCF) compared to the theoretical X-ray diffraction pattern of MOF-5 can indicate the presence of guest molecules (palladium nanoparticles) in the pores of the metal-organic framework. On the contrary, in the case of composite samples **I** and **III** (impregnation from $\text{Pd}(\text{acac})_2$), it can be suggested that palladium nanoparticles are located on the external surface of crystallites of the metal-organic framework.

The characteristic reflections of PdO and $\text{Pd}(\text{OAc})_2$ are absent from the X-ray diffraction patterns of the Pd@MOF-5 samples. According to the EXAFS data,

palladium is fully reduced in the studied materials. It is most likely that the precursor is completely decomposed to form Pd^0 nanoparticles when the palladium-containing materials are prepared.

The influence of the method of catalyst preparation on the palladium particle size in the metal-organic structure of MOF-5 was studied by a combination of XAS and HR TEM methods. The processing of the EXAFS spectra by the spherical approximation method indicates a very small average diameter of the palladium particles in the samples with the metal-organic framework. The EXAFS spectra of all samples contain a peak at the uncorrected distance from the central Pd atom near 1.5 \AA . The peak in the spectrum of palladium oxide is at the same distance and is attributed to the atomic pair Pd—O and/or Pd—C. The second peak at the distance about 2.5 \AA can be assigned to the presence of the atomic pair Pd—Pd. Assuming the spherical shape of the particles, we can calculate the formal average diameter of metallic palladium particles. The calculation shows that nanoparticles with sizes about 1 nm result from the reduction of the precursor on the MOFs surface. The size of particles immobilized in the metal-organic framework matrix depends on the preparation method and palladium precursor. So, very small (0.5 nm) palladium particles are formed in the MOF-5 matrix of samples **I**. Larger particles (0.6 nm , Table 2) are immobilized in the matrix of sample **III** prepared by impregnation from palladium acetylacetonate. When preparing palladium-containing sample **V** (3.5% Pd) in supercritical CO_2 , the average size of the palladium nanoparticles attains values of $1.2\text{--}1.4 \text{ nm}$.

The HR TEM studies of palladium-containing samples Pd@MOFs indicate the presence of small Pd nanoparticles (about 1 nm) in sample **I** (Fig. 4, a). Larger palladium nanoparticles (to 2 nm , Fig. 4, b) are formed in sample **III**. A comparison of these data with the XRF results suggests that smaller palladium particles are formed in the case of catalyst **I** (Pd acetate as a precursor). In sample **III** (Pd acetylacetonate as a precursor), the bimodal nanoparticle-size distribution is observed: along with small particles (0.6 nm , see Table 2), the palladium-containing system also contains larger particles ($1.5\text{--}2 \text{ nm}$). Probably, the content of smaller particles considerably exceeds the amount of larger particles. This follows from

Table 2. Parameters of composite samples Pd@MOF-5 obtained by the EXAFS method

Sample	Pair	$r/\text{\AA}$	CN*	$\sigma^2 \cdot 10^{-3} / \text{\AA}^2$	$\Delta E / \text{eV}$	$D_{\text{Pd}}/\text{\AA}$
I	Pd—Pd	2.74 ± 0.04	3.5 ± 0.2	12 ± 1	2 ± 1	5.2 ± 0.4
III	Pd—Pd	2.76 ± 0.03	4.3 ± 1.0	9 ± 4	5 ± 2	6.1 ± 0.6
V	Pd—Pd	2.75 ± 0.01	8.1 ± 0.6	6 ± 1	1 ± 1	12.4 ± 2.4

CN is coordination number.

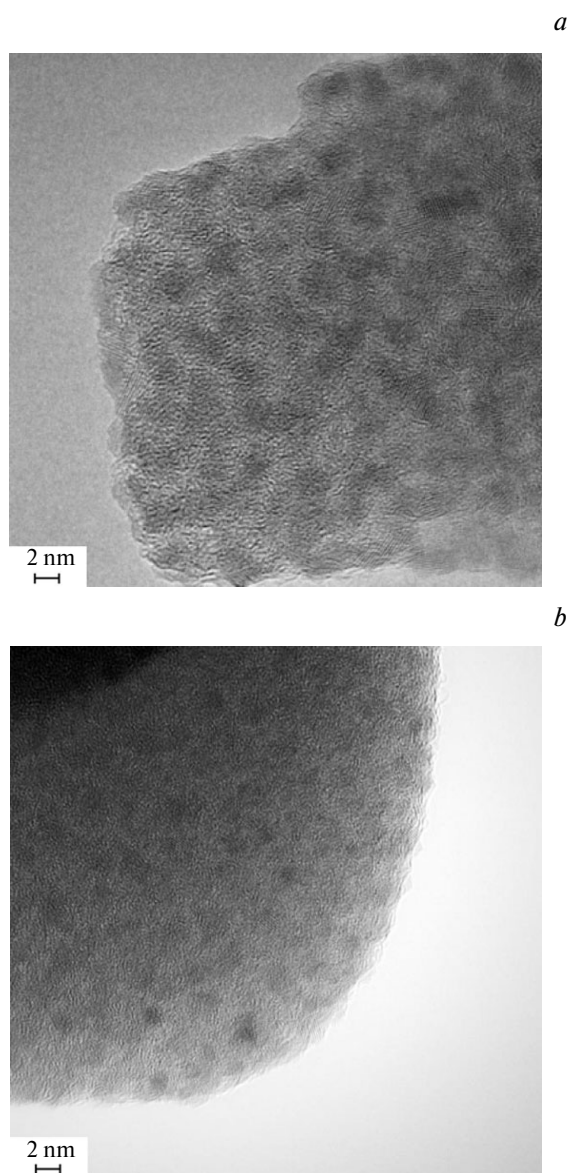


Fig. 4. TEM images of palladium-containing samples **I** (a) and **III** (b) prepared by the impregnation to incipient wetness method.

the principal approaches on which two complementary methods, HR TEM and XRF, are based.

Catalytic properties of the synthesized composite materials Pd@MOF-5. The synthesized composites Pd NPs@MOF are highly active in the partial hydrogenation of phenylacetylene to styrene (Table 3, Fig. 5). The highest rate for phenylacetylene hydrogenation is achieved in the presence of catalyst **III** prepared by the impregnation to incipient wetness method using palladium acetylacetonate. The use of the palladium-containing system prepared by impregnation from palladium acetate (sample **I**) noticeably decreases the hydrogenation rate of an acetylene compound. A sharp decrease in the phenylacetylene hydrogenation rate is observed in the presence of the pal-

Table 3. Rates (W_{01} , W_{02}) and selectivity (S) at the initial step of the partial hydrogenation of phenylacetylene on palladium-containing composites Pd/MOF-5

Catalyst	W_{01}	W_{02}	S_1^a	S_2^b
	mol (mol min) ⁻¹			
I	11.6	47.9	98	97
II	9.9	17.7	97	95
III	45.6	96.3	92	86
IV	6.0	0.2	95	90
V	13.7	0.5	94	92

Note. Reaction conditions: 100 mg of the catalyst, 460 mg of phenylacetylene, and 20 mL of methanol; 1 atm H₂, 20 °C; selectivity at phenylacetylene conversions of 50% (S_1) and 90% (S_2) conversion, respectively.

ladium-containing materials prepared in SCF (samples **IV** and **V**, see Table 3).

As follows from Scheme 1, phenylacetylene hydrogenation proceeds in two steps: at first phenylacetylene is hydrogenated to styrene, which corresponds to the consumption of the first mole of hydrogen, and then styrene is converted to ethylbenzene when the second mole of hydrogen is consumed. The ratio of hydrogenation rates of acetylene and monoene is substantial for the isolation of the target product upon the partial reduction of polyunsaturated compounds.⁴⁷

It is known that the selectivity of partial hydrogenation of compounds with the multiple C—C bond to monoene in the presence of the palladium-containing catalysts is determined by two factors: (1) mechanism of hydrogen addition to acetylene/diene compound (selectivity by mechanism) and (2) adsorption displacement at which adsorption of polyunsaturated compound prevents re-adsorption of alkene (thermodynamic factor of selectivity).⁴⁸ The selectivity at the first step of hydrogenation to

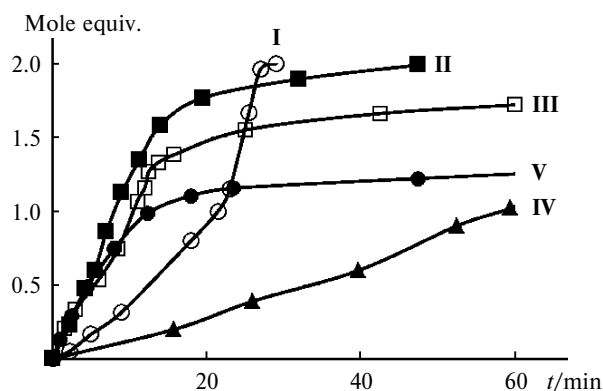


Fig. 5. Kinetic curves of the partial hydrogenation of phenylacetylene on synthesized palladium-containing samples Pd@MOF-5 **I–V**. Mole equiv. is the mole equivalent of absorbed H₂.

styrene is determined by the mechanism of hydrogen addition to phenylacetylene. Adsorption displacement is the thermodynamic factor of selectivity and determines the rate for styrene hydrogenation at the end of the first step and at the second step. In the presence of the Pd@MOF-5 samples prepared by impregnation to incipient wetness, the hydrogenation rate at the second step substantially increases, most likely, due to a decrease in the strength of styrene adsorption on the metal-organic framework after the complete conversion of phenylacetylene (see Table 3). As the palladium content increases, the rate of styrene conversion to ethylbenzene decreases sharply in the presence of the Pd@MOF-5 sample prepared by impregnation from palladium acetate (sample **II**).

The optimum ratio of the hydrogenation rates of phenylacetylene and styrene to ethylbenzene is achieved in the presence of catalysts **IV** and **V** prepared in SCF. In this case, the hydrogenation of styrene to ethylbenzene is nearly completely suppressed (see Table 3).

The observed differences in activity of the obtained catalysts in the partial hydrogenation of phenylacetylene are probably related to the dispersion and localization of palladium nanoparticles in the MOF-5 matrix.

Several authors reported that the reaction rate decreases with an increase in the dispersion of the metal.³⁰ The effect of the metal particle size in the case of alkyne hydrogenation on the palladium-containing catalysts is that the selectivity and activity decrease with an increase in the dispersion of the metal.⁴⁹ We have recently showed that the activity in the hydrogenation of butynediol-1,4 on the palladium-containing MOFs increases with an increase in the Pd nanoparticle size.⁵⁰

A comparison of the results of catalytic experiments and XRF and TEM data reveals a correlation between the size of palladium particles localized on the support surface and the activity of the obtained catalysts. Sample **I** with the smallest average particle diameter (0.52 nm according to the XRF data or less than 1 nm according to the HR TEM data) exhibits the lowest activity in the partial hydrogenation of phenylacetylene to styrene (see Table 3).

An increased activity of system **III** compared to sample **I** is due to the accessibility of active sites, *i.e.*, their immobilization on the external surface of the metal-organic framework, and to the formation of larger palladium particles (0.6 nm according to the XRF data or 1.5–2 nm according to the HR TEM data). In the case of systems **IV** and **V** prepared in a medium of SCF, the active sites are predominantly immobilized, most likely, in pores of the metal-organic framework. Thus, taking into account the pore size accessible for the adsorbate in the metal-organic framework MOF-5 equal to 1.2–1.5 nm, samples **I** and **III** should be ascribed to class **A** (according to R. A. Fischer's terminology⁵) and samples **IV** and **V** are attributable to class **B** (or **C**).

The selectivity of the obtained catalysts toward styrene depends substantially on several factors: the nature of the precursor, method of precursor introduction, and palladium content in the MOF-5 matrix. To the end of the first step of hydrogenation palladium-containing samples **IV** and **V** prepared in SCF demonstrate selectivity higher than 90% (see Table 3). The highest selectivity ($S_1 \sim 98\%$) for the partial hydrogenation of phenylacetylene is observed in the presence of catalyst **I** prepared by the impregnation to incipient wetness method from palladium acetate (see Table 3, conversion of phenylacetylene 50%). To the end of consumption of the first mole of hydrogen (conversion of phenylacetylene 95%) the selectivity of this system remains high ($S_2 \sim 97\%$, see Table 3). As the palladium content in this system increases to 5 wt.% (catalyst **II**), the selectivity remains almost unchanged ($S_1 \sim 97\%$, conversion of phenylacetylene 50%). In this case, an insignificant decrease in the selectivity ($S_2 \sim 95\%$) is observed to the end of the first hydrogenation step (see Table 3). The replacement of palladium acetate by Pd(acac)₂ in the case when impregnation to incipient wetness was used results in a noticeable decrease in the selectivity for styrene on palladium-containing material **III** ($S_2 \sim 86\%$ at 95% conversion). Probably, the formation of larger palladium particles in the Pd@MOF-5 system, the possible bimodal nanoparticle size distribution (see above) and the ensuing heterogeneity of active sites result in a decrease in the selectivity for monounsaturated compound. Catalysts **IV** and **V** prepared in supercritical CO₂ using the same precursor (palladium acetylacetonate) are characterized by a higher selectivity of 90–92% (conversion of phenylacetylene 95%) for styrene compared to sample **III**. Most likely, this is related to the presence of active sites in pores of these Pd@MOF-5 samples prepared in SCF and to the assumed monomodal size distribution of palladium nanoparticles (characteristic of the introduction of metal under the fluid synthesis conditions). Thus, the selectivity of the synthesized palladium-containing materials Pd@MOF-5 is probably determined by differences in dispersion and position of palladium nanoparticles affected by the preparation method of the catalytic system.

The obtained palladium-containing materials Pd@MOF-5 are stable in the studied reaction. For example, in the presence of sample **III**, the initial specific hydrogenation rate of phenylacetylene to styrene (W_{01}) remained unchanged within three cycles (Fig. 6). Upon the multiple use of this catalyst, the rate of the undesirable styrene conversion to ethylbenzene (W_{02}) decreases noticeably.

Thus, the palladium-containing systems involving small Pd nanoparticles (less than 2 nm) immobilized in the matrix of the microporous phenylenecarboxylate metal-organic framework MOF-5 were synthesized for the first time by the fluid synthesis method. The activity and selectivity of the Pd@MOF-5 catalysts in the partial hydro-

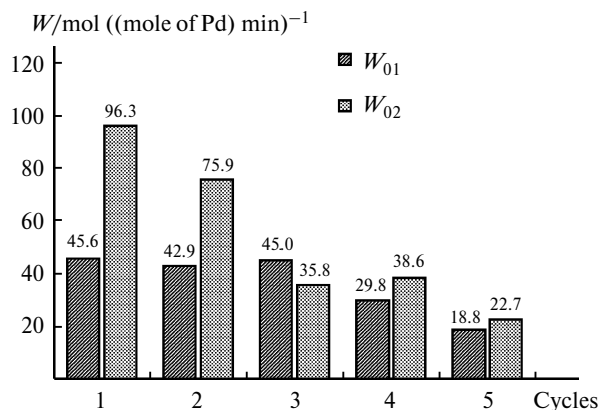


Fig. 6. Stability of palladium-containing sample MOF-5 in the partial hydrogenation of phenylacetylene; W_{01} and W_{02} are the initial specific rates for the hydrogenation of phenylacetylene and styrene, respectively.

generation of phenylacetylene depend substantially on the preparation method (fluid synthesis in supercritical CO_2 and impregnation to incipient wetness) and on the nature of the palladium precursor. A comparison of the catalytic experimental data and results of physicochemical studies suggested that small palladium nanoparticles (about 1–2 nm) are predominantly immobilized in pores of the metal-organic framework of composite material 1%Pd@MOF-5 synthesized in supercritical CO_2 . This position of active sites favors the suppression of the undesirable styrene conversion to ethylbenzene. The highest selectivity for styrene (~95–97% at a phenylacetylene conversion of 95%) is observed in the presence of palladium-containing materials 1%Pd@MOF-5 and 5%Pd@MOF-5 prepared by the impregnation to incipient wetness method from palladium acetate. The development of the composite materials, being palladium nanoparticles immobilized in the matrix of the metal-organic framework MOF-5, makes it possible to control the catalytic properties of the Pd@MOF-5 system in the partial hydrogenation of acetylene compounds.

This work was financially supported by the Russian Russian Foundation for Basic Research (Project No. 12-03-01097-a).

References

- V. I. Párvulescu, C. Hardacre, *Chem. Rev.*, 2007, **107**, 2615.
- J. Silvestre-Albero, F. Rodriguez-Reinoso, A. Sepulveda-Escribano, *J. Catal.*, 2002, **210**, 127.
- S. R. de Miguel, M. C. Roman-Martinez, D. Cazorla-Amoros, E. L. Jablonski, O. A. Scelza, *Catal. Today*, 2001, **66**, 289.
- S. Turner, O. I. Lebedev, F. Schröder, D. Esken, R. A. Fischer, G. Van Tendeloo, *Chem. Mater.*, 2008, **20**, 5622.
- M. Meilikhov, K. Yusenko, D. Esken, S. Turner, G. Van Tendeloo, R. A. Fischer, *Eur. J. Inorg. Chem.*, 2010, 3701.
- D. Farrusseng, S. Aguado, C. Pinel, *Angew. Chem., Int. Ed.*, 2009, **48**, 7502.
- M. Sabo, A. Henschel, H. Frode, E. Klemm, S. Kaskel, *J. Mater. Chem.*, 2007, **17**, 3827.
- H.-L. Jiang, B. Liu, T. Akita, M. Haruta, H. Sakurai, Q. Xu, *J. Am. Chem. Soc.*, 2009, **131**, 11302.
- H.-L. Jiang, T. Akita, T. Ishida, M. Haruta, Q. Xu, *J. Am. Chem. Soc.*, 2011, **133**, 1304.
- S. Hermes, F. Schröder, S. Amirjalayer, R. Schmid, R. A. Fischer, *J. Mater. Chem.*, 2006, **16**, 2464.
- F. Schröder, D. Esken, M. Cokoja, M. W. E. van den Berg, O. I. Lebedev, G. Van Tendeloo, B. Walaszek, G. Buntkowsky, H.-H. Limbach, B. Chaudret, R. A. Fischer, *J. Am. Chem. Soc.*, 2008, **130**, 6119.
- K. Park, S. B. Choi, H. J. Nam, D.-Y. Jung, H. C. Ahn, K. Choi, H. Furukawa, J. Kim, *Chem. Commun.*, 2010, **46**, 3086.
- H.-L. Jiang, Q. Xu, *J. Mater. Chem.*, 2011, **21**, 13705.
- X. Gu, H.-L. Jiang, T. Akita, Q. Xu, *J. Am. Chem. Soc.*, 2011, **133**, 11822.
- A. Bayrakçeken, B. Cangül, L. C. Zhang, M. Aindow, C. Erkey, *Int. J. Hydrogen Energy*, 2010, **35**, 11669.
- B. Cangül, L. C. Zhang, M. Aindow, C. Erkey, *J. Supercrit. Fluids*, 2009, **50**, 82.
- A. Bayrakçeken, A. Smirnova, U. Kitkamthorn, M. Aindow, L. Turker, I. Eroglu, C. Erkey, *Chem. Eng. Commun.*, 2009, **196**, 194.
- Y. Zhang, B. Cangul, Y. Garrabos, C. Erkey, *J. Supercrit. Fluids*, 2008, **44**, 71.
- C. Erkey, *J. Supercrit. Fluids*, 2009, **47**, 517.
- A. Bayrakçeken, A. Smirnova, U. Kitkamthorn, M. Aindow, L. Turker, I. Eroglu, C. Erkey, *J. Power Sources*, 2008, **179**, 532.
- A. Bayrakçeken, A. Smirnova, U. Kitkamthorn, C. Erkey, *Scripta Mater.*, 2007, **56**, 101.
- Y. Zhang, C. Erkey, *J. Supercrit. Fluids*, 2006, **38**, 252.
- R. Jiang, Y. Zhang, S. Swier, *Electrochem. Solid State Lett.*, 2005, **8**, 611.
- Y. Zhang, D. Kang, C. Saquing, M. Aindow, C. Erkey, *Ind. Eng. Chem. Res.*, 2005, **44**, 4161.
- S. Solodovnikov, A. Vasil'kov, A. Olenin, E. Titova, V. Sergeev, *Dokl. Chem. (Engl. Transl.)*, 1990, **310** [*Dokl. Akad. Nauk SSSR*, 1990, **310**, 912].
- A. Vasil'kov, A. Olenin, E. Titova, V. Sergeev, *J. Colloid Interface Sci.*, 1995, **169**, 356.
- Y. Zhao, J. Zhang, J. Song, J. Li, J. Liu, T. Wu, P. Zhang, B. Han, *Green Chem.*, 2011, **13**, 2078.
- T. Wu, P. Zhang, J. Ma, H. Fan, W. Wang, T. Jiang, B. Han, *Chin. J. Catal.*, 2013, **34**, 167.
- E. J. Beckman, *J. Supercrit. Fluids*, 2004, **28**, 121.
- A. Molnar, A. Sarkany, M. Varga, *J. Mol. Catal. A*, 2001, **173**, 185.
- M. L. Derrien, *Stud. Surf. Sci. Catal.*, 1986, **27**, 613.
- H. Arnold, F. Dobert, J. Gaube, in *Handbook of Heterogeneous Catalysis*, Eds G. Ertl, H. Knözinger, J. Weitkamp, VCH, Weinheim, 1997, p. 2165.
- H. D. Neubauer, A. Heilmann, J. Kötter, R. Schubert, *Tagungsbericht*, 1993, **9305**, 67.
- S. Dominguez-Dominguez, A. Berenguer-Murcia, A. Linares-Solano, D. Cazorla-Amoros, *J. Catal.*, 2008, **257**, 87.
- T. Vergunst, F. Kapteijn, J. A. Moulijn, *Ind. Eng. Chem. Res.*, 2001, **40**, 2801.

36. X. Huang, B. Wilhite, M. J. McCready, A. Varma, *Chem. Eng. Sci.*, 2003, **58**, 3465.
37. J. Panpranot, K. Phandinthong, T. Sirikajorn, M. Arai, P. Praserthdam, *J. Mol. Catal. A: Chem.*, 2007, **261**, 29.
38. R. Tschan, R. Wandeler, M. S. Schneider, M. M. Schubert, A. Baiker, *J. Catal.*, 2001, **204**, 219.
39. J.-L. Pelegatta, C. Blandy, V. Colliere, R. Choukroun, B. Chaudret, P. Cheng, K. Philipot, *J. Mol. Catal. A: Chem.*, 2002, **178**, 55.
40. D. J. Tranchemontagne, J. R. Hunt, O. M. Yaghi, *Tetrahedron*, 2008, **64**, 8553.
41. A. L. Klyachko-Gurvich, *Bull. Acad. Sci. USSR, Div. Chem. Sci. (Engl. Transl.)*, 1961, **10** [*Izv. Akad. Nauk SSSR, Ser. Khim.*, 1961, **10**, 1884].
42. A. S. Kashin, V. P. Ananikov, *Russ. Chem. Bull. (Int. Ed.)*, 2011, **12**, 2551 [*Izv. Akad. Nauk, Ser. Khim.*, 2011, **12**, 2551].
43. J. Kim, D. O. Kim, D. W. Kim, K. Sagong, *J. Solid State Chem.*, 2013, **197**, 261.
44. V. B. Fenelonov, *Poristy uglerod [Porous Carbon]*, Novosibirsk, 1995, 513 pp. (in Russian).
45. P. J. Hagrman, D. Hagrman, J. Zubieta, *Angew. Chem., Int. Ed.*, 1999, **38**, 2638.
46. J. Havicovic, M. Bjorgen, U. Olsbye, P. D. C. Dietzel, S. Bordiga, C. Prestipino, C. Lamberti, K.-P. Lillerud, *J. Am. Chem. Soc.*, 2007, **129**, 3612.
47. H. Lindlar, *Helv. Chim. Acta*, 1952, **35**, 446.
48. G. C. Bond, G. Webb, P. B. Wells, J. M. Winterbottom, *J. Catal.*, 1962, **1**, 74.
49. J. P. Boitiaux, J. Cosyns, S. Vasudevan, *Appl. Catal.* 1983, **6**, 41.
50. V. Isaeva, O. Tkachenko, E. Afonina, G. I. Kapustin, W. Grunert, S. E. Solov'eva, I. S. Antipin, L. Kustov, *Micropor. Mesopor. Mater.*, 2013, **166**, 167.

Received November 15, 2013;
in revised February 6, 2014